Natural Product Reports

ROYAL SOCIETY OF CHEMISTRY

REVIEW

View Article Online
View Journal

Cite this: DOI: 10.1039/d6np00006a

High-throughput assays for SAM-dependent methyltransferases: advances, challenges, and future perspectives

Renia Fotiadou, [a] Florian Heinz,[b] Konstantin F. G. Weigmann, [b] Mark Doerr,[b] Uwe T. Bornscheuer *[b] and Ioannis V. Pavlidis *[a]

Covering: up to January 2026

Methyltransferases (EC 2.1.1.–) represent one of the most functionally diverse enzyme families in biology. Found across all domains of life—including bacteria, archaea, eukaryotes, and viruses—these enzymes catalyze a wide range of methylation reactions, commonly on *O*-, *N*-, and *C*-atoms, in a chemo- and regioselective manner. The wide set of substrates methylated is why a universal assay for the methyltransferase's activity screening has not yet been established. Despite this diversity, most methyltransferases utilize a common methyl donor, the *S*-adenosyl-L-methionine (SAM). This shared feature has enabled the development of several assay strategies based on the detection of *S*-adenosyl-L-homocysteine, the by-product of SAM-dependent methylation, or its degradation products. Colorimetric and fluorometric assays have been widely employed to monitor methyltransferase activity, each with distinct advantages and limitations, depending on the substrate/product detection of the methylation reaction, but also whether they require purified enzymes or work in crude (*E. coli*) cell lysates. However, the methylation of substrates with more than one nucleophilic atom requires sophisticated analytical tools for accurate monitoring of the regiospecificity of methyltransferases. This complexity often limits the broader exploitation of methyltransferases, particularly in enzyme engineering efforts, where large datasets are generated and must be efficiently analyzed. This review critically examines the high-throughput screening assays developed to date for methyltransferase activity.

Received 21st January 2026

DOI: 10.1039/d6np00006a

rsc.li/npr

[a]Department of Chemistry, University of Crete, Voutes University Campus, 70013 Heraklion, Greece. E-mail: ipavlidis@uoc.gr

[b]Department of Biotechnology & Enzyme Catalysis, Institute of Biochemistry, University of Greifswald, Felix-Hausdorff-Str. 4, D-17487 Greifswald, Germany. E-mail: uwe.bornscheuer@uni-greifswald.de

1. Introduction

1.1. Biological and pharmaceutical relevance of SAM-dependent methyltransferases

S-Adenosyl-L-methionine (SAM)-dependent methyltransferases (MTs) represent the largest and most diverse group of MTs (EC 2.1.1.–). SAM-MTs facilitate the transfer of a methyl group from SAM to a broad variety of acceptor substrates/nucleophiles, ranging from small molecules to biomacromolecules, while *S*-adenosyl-L-homocysteine (SAH) is formed as a by-product (Fig. 1). MTs can methylate various atoms, with *O*-, *N*-, and *C*-methylation being the most common ones. Methylation reactions are found across all domains of life, playing a pivotal role in intercellular processes and the synthesis of small molecules

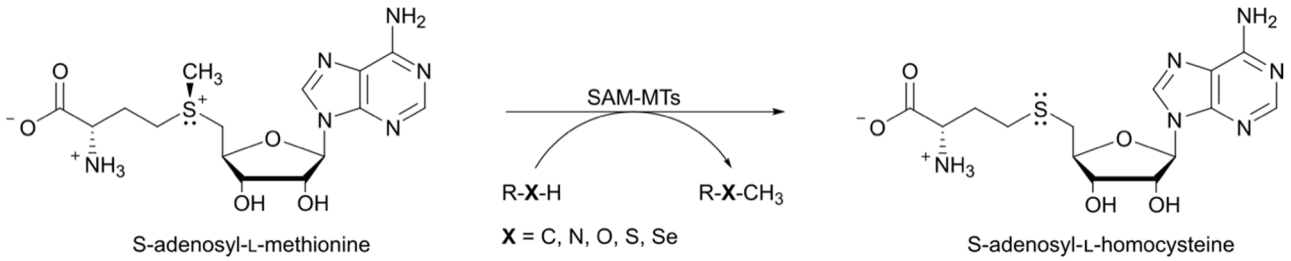

Fig. 1 SAM is used as universal methyl donor from SAM-dependent MTs, transferring this group to small molecules, proteins or DNA. SAM-MTs exhibit high chemoselectivity, targeting *C*-, *N*-, *O*-, *S*-, or *Se*-atoms, while the transfer leaves SAH as a by-product.

and metabolites.[1] The strict intracellular regulation of SAM-MTs expression and activity is critical, since deviant methylation is associated with diseases, including cancer, neurodegeneration, and autoimmune disorders.[2,3] For instance, catechol-*O*-MTs (COMT) methylate catecholamines, and thus regulate neural signalling and stress response; increased activity of these SAM-MTs can lead to mental health conditions.[2] Synthesis of melatonin by *N*-acetylserotonin *O*-MT regulates the circadian rhythm.[3] Histamine *N*-MT inactivates histamine in order to regulate physiological responses, such as inflammation, immune responses *etc.*, by methylating it.[2]

It is clear through these examples that the precise regulation of MTs is of utmost importance for human health, and that MTs are attractive pharmacological targets. Nevertheless, SAM-MTs are at the same time exceptional biocatalysts for synthesizing methylated derivatives of compounds of interest. The increasing interest in this particular activity is associated with the well-described "magic methyl effect".[4] The methylation of even one functional group, such as –OH or –NH, can significantly influence the lipophilicity, electron distribution, stereochemistry, and stability of a molecule, which, in turn, strongly affects the bioavailability, tissue distribution, half-life, and potency of potential drugs, inhibitors, or modulators. SAM-MTs catalyze these reactions efficiently under mild, aqueous, and physiologically relevant conditions, making them highly attractive catalysts compared to the chemical alternatives.[5]

Many research groups investigated the synthetic potential of SAM-MTs, particularly natural product MTs (NPMTs), for producing methylated compounds with desired biological activities. Inspired by the natural role of NPMTs, several researchers have synthesized in scalable quantities *O*- or *N*-methyl derivatives of flavonoids, alkaloids and phenolic acids, exhibiting antioxidant, antibacterial, and anti-inflammatory activities, and thus providing significantly higher amounts than those obtained when isolated from natural sources, such as plants.[6–9] Among these products, there are several with significant biological activities. Methylated derivatives of key flavones have demonstrated strong inhibitory effects against carcinogen-activating cytochrome P450.[10] Moreover, methylation of alkaloids leads to active pharmaceutical ingredients targeting pain, infectious diseases, metabolic disorders, and more.[11] *C*-MTs are quite important synthetically, as, apart from being able to form C–C bonds with non-activated atoms, they expand the chemical space of terpenes, by introducing methyl groups at specific carbon positions.[12] The applications of SAM-MTs also extends into the food industry, where regiospecific SAM-MTs can synthesize methylated compounds that can be used to improve sensory profiles of food products;[13,14] an example is the enzymatic production of vanillin *via* regioselective *O*-methylation of protocatechuic aldehyde.[15,16] Very recently, Chapple *et al.* used the *N*-methyltransferase SgPsmC from *Streptomyces griseofuscus* for the selective kinetic resolution of pyrroloindolines, which are structural elements of a variety of alkaloids with biological activities.[17] SgPsmC was found to be selective against several substrates, providing only one diastereomer, while the process could be scaled-up to laboratory preparative scale (50 mg). The reviews of Struck *et al.*[18] and Abdelraheem *et al.*[19] comprehensively discuss and highlight the applications of several SAM-MTs in biocatalysis and biosynthetic routes.

1.2. Diversity and mechanisms of SAM-dependent methyltransferases

SAM-MTs exhibit remarkable diversity in their structural folds and catalytic mechanisms, providing a versatile platform for regio- and stereoselective methylations of different molecules/nucleophiles. Their ability to catalyze methylation reactions on both natural and non-natural compounds significantly expands their utility and biological relevance, enabling greener and more versatile synthetic routes compared to the established chemical ones. A short introduction on the classification and mechanisms of SAM-MTs is provided in the following paragraphs. It should be noted that radical SAM or carboxy-SAM-dependent MTs are not covered in this review.

1.2.1. Classification of SAM-dependent methyltransferases. Canonical SAM-MTs are classified based on the nucleophile atom, typically *C*–, *O*–, *N*–, *S*– and *Se*–, or even halides and thiocyanates, to which a methyl group is transferred.[20] *O*-MTs and *N*-MTs are found across all domains of life and constitute up to 78% of the recorded MTs. They target small metabolites to macromolecules, explaining their wide diversity and for their biocatalytic applications they are the most studied MTs. *C*-MTs and halide-MTs are mainly found in bacteria, plants, and yeast or fungi, respectively; whereas *S*-MTs and *Se*-MTs are common in plants, mammals and certain bacteria.[20,21] However, certain MTs can transfer a methyl group to more than one nucleophile.[22]

Certain classifications of SAM-MTs rely on their amino acid sequence, their mode of SAM binding, or their tertiary/

quaternary structure. Specific motifs and architectural features unveiled through sequence alignment have led to the categorization of SAM-MTs into five distinct Classes (I–V). The most common and largest group is Class I MTs, including most *O*- and *N*-MTs, characterized by the Rossmann-like fold (alternating β-strands and α-helices arranged to bind nucleotide cofactors; a three-layered $\alpha/\beta/\alpha$ topology).[23] They occur as monomers, dimers, and tetramers targeting small molecules, proteins, lipids, and nucleic acids.[24–26] As the sequence space is being explored, additional categories have emerged with structural characteristics distinct from those of the original classification (*e.g.*, radical SAM-MTs, transmembrane MTs, *etc.*).[20] The architectural features of Class I–V MTs are thoroughly discussed by Liscombe *et al.*[20] and Schubert *et al.*[27] and they will not be further discussed here.

1.2.2. Mechanisms of SAM-dependent methyltransferases. The vast majority of known MTs use SAM as a methyl donor due to its abundance in biological systems, and the favourable thermodynamics ($\Delta G < 0$) for the transfer of the methyl group.[28,29] This is derived from the charged methylsulfonium center; the sulfonium ion carries a net positive charge, rendering the adjacent methyl carbon highly electrophilic and susceptible to nucleophilic attack, leading to an S_N2-type reaction.[27] For SAM-dependent methylation to proceed, the methyl group donor and the substrate's methyl acceptor atom must be properly aligned.[20] Briefly, S_N2-like methylation takes place through three distinct mechanisms: (i) proximity and desolvation (removal of surrounding water to increase nucleophile strength and local concentration),[30] (ii) acid/base *trans*-methylation (activation of the nucleophile by conserved basic amino acids; proton shuttle system),[31] and (iii) metal-based (coordination/stabilization of the nucleophile or influence its pK_a by divalent cations to promote deprotonation).[32,33] The structure of SAM secures precise proper positioning in the active site of the enzyme, and intermolecular interactions with potential substrates. The compounds to be methylated are coordinated in the active site *via* interactions with the side chains for the amino acids of the area, the adenosyl moiety of SAM, and the reactive group.[18,34] A mechanistically unique superfamily known as the radical SAM-MTs have been classified, which facilitate the methylation of weakly nucleophilic or non-activated sites *via* a $[Fe_4S_4]^{2+}$ cluster. This class has been thoroughly discussed by Booker *et al.*[35] and will not be covered in this review.

The strong reactivity of SAM renders it prone to degradation under physiological and process conditions. Consequently, biocatalytic applications often require it to be supplied in excess or step-wise, to maintain adequate SAM levels during the bioprocess. For this purpose, several approaches have been developed to produce SAM *in situ*. Enzymatic synthesis offers the major advantage of providing stereoselectivity at the sulfur atom, albeit in several cases it is accompanied with greater complexity. The balance of yield, selectivity, cost-effectiveness, and operational simplicity yet remains a significant challenge. Special focus has also been given to the synthesis of SAM analogues in order to (i) produce more stable SAM derivatives (*e.g.*, SAM carboxylate isosteres – tetrazolates) and (ii) enable different alkylations beyond methylation (*e.g.*, ethylation *via* the use of *S*-adenosyl-L-ethionine).[36–40]

Research on SAM-MTs nowadays focuses on addressing major questions such as: (a) how we can identify new MTs or guide their enzyme engineering from data available in protein sequence databases, (b) how can we expand the scope of the products formed, *i.e.*, substrate scope and alternative alkylations, and (c) how can SAM-MTs biocatalytic reactions be scaled-up. Especially for the first two queries, suitable and universal high-throughput assays are pivotal to identify and improve desired enzyme candidates. In the following chapter we summarize and critically evaluate the assays developed to evaluate SAM-dependent MTs. A concise table summarizing all following assays, including the detected compound for each (as most are indirect), is provided in the SI.

2. High-throughput assays for SAM-dependent methyltransferases

2.1. Colorimetric assays

Historically, the biochemical characterization of MT relied on biochemical assays in tissue extracts using radiolabelled methyl donors,[41] progressing later to more advanced and safer technologies to analyse MT activity. Spectrophotometric assays rely on the measurement of changes in absorption correlated to the conversion of the substrate by the enzyme (Fig. 2).[42] In general, these assays offer advantages, such as low cost and operational simplicity. To overcome several challenges that arose—such as minimal differences in absorption between methylated and non-methylated compounds—more sensitive chromogenic substrate and enzyme-coupled strategies have been developed. Such enhancements improved the detection limit and enabled reliable and sensitive spectrophotometric detection of MT activity.

One of the earliest assays for the characterization of a COMT took advantage of shifts in spectrophotometric properties of 3,4-dihydroxyacetophenone upon methylation, though this

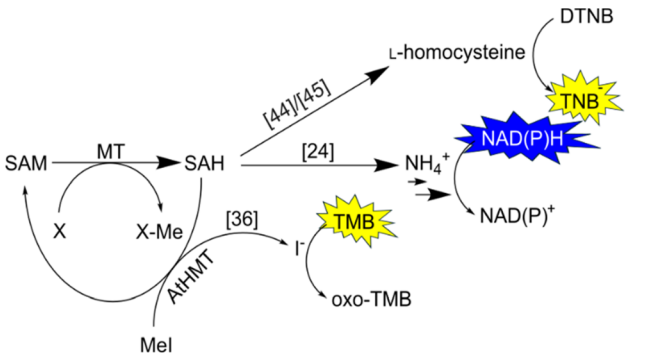

Fig. 2 Spectrophotometric assays for determining SAM-dependent methyltransferase activity. Example I/II: detection of L-homocysteine released from SAH *via* reduction of 5,5′ dithio-bis-(2-nitrobenzoic acid) (DTNB) to 2-nitro-5-thiobenzoic acid (TNB).[44,45] Example III: enzyme-coupled detection of SAH *via* oxidation of NAD(P)H.[24] Example IV: detection of 3,3′,5,5′-tetramethylbenzidine (TMB) oxidation *via* HOI generated by chloroperoxidase.[36]

approach was limited by significant methodological drawbacks, such as the spectral change being dependent on the *meta*/*para* ratio of the products.[43] A pivotal development was the universal assay developed by Hendricks *et al.*, which involves the enzymatic hydrolysis of SAH by a SAH nucleosidase,[44] as it circumvents product inhibition from SAH. Subsequent conversion of *S*-ribosylhomocysteine by an *S*-ribosylhomocysteine lyase (LuxS) enabled quantification of released L-homocysteine using Ellman's reagent, 5,5′-dithio-bis-(2-nitrobenzoic acid) (DTNB, Fig. 2-I) at 412 nm with a detection limit of 4 μM SAH. This allowed to determine the kinetic parameters for a salicylic acid carboxyl methyltransferase after purification. Schäberle *et al.* streamlined this workflow (Fig. 2-II) by applying a SAH hydrolase (SAHH) to release L-homocysteine directly from SAH, thus eliminating the need of a prior adenine cleavage and utilized this to characterize a putative MT from the bacterium *Herpetosiphon* sp. B060.[45] While the absorbance shift to 412 nm permits measurement in 96-well polystyrene plates, the discontinuous assay format required a one-hour incubation time before measurement. The assay may be performed with crude protein extracts, but cysteine residues present in proteins and other thiols can lead to increased background signal; thus, proper standards are crucial for the evaluation of the applicability of the assay before the screening.

Dorgan *et al.* further advanced this assay design by implementing a continuous measurement, in which an SAH nucleosidase liberates adenine that is subsequently deaminated from adenine deaminase to hypoxanthine and ammonia, resulting in a decrease in absorbance at 265 nm.[46] Their assay was demonstrated for rat protein arginine *N*-MT 1 using three different peptide substrates to determine kinetic parameters. As this wavelength is prone to background interference (from *e.g.* proteins present in crude cell lysate, interference with cuvettes' or microtiter plates' material), Duchin *et al.* coupled ammonia release to NAD(P)H oxidation, catalyzed by a glutamate dehydrogenase (Fig. 2-III), first demonstrated in 2015 for protein lysine MT SET7/9 and SETD6, and DNA MT M.HaeIII from *Haemophilus aegyptius*.[24] In this approach, a glutamate dehydrogenase utilizes the ammonia to form glutamate from α-ketoglutarate thus oxidizing NAD(P)H and enabling monitoring at 340 nm. This improved sensitivity, enabling detection of SAH concentrations as low as 170 nM, though the involvement of three additional enzymes increased assay complexity.

A more streamlined high-throughput continuous spectrophotometric assay was introduced in 2022, utilizing a SAH deaminase, instead of a SAH nucleosidase/adenine deaminase coupling.[47] Apart from the applicability of the assay for the indirect detection of MT activity, the inhibition of the MTs by the formed *S*-inosylhomocysteine (SIH) was investigated; no inhibition was observed for COMT, as well as for the SafC *O*-MT[48] and a *N*-MT from *Ruta graveolens*.[49]

A different enzyme-coupled approach for SAH detection was described by Kailing *et al.*[50] In this assay, the reaction cascade is initiated by the SAH hydrolase, which cleaves SAH to adenosine and homocysteine. The resulting adenosine is subsequently phosphorylated by adenosine kinase to yield AMP, generating equimolar amounts of ADP. ATP regeneration is then mediated by a pyruvate kinase, which converts phosphoenolpyruvate to pyruvate. The latter is then reduced to lactate by a lactate dehydrogenase, enabling spectrophotometric monitoring of the decrease in absorbance at 340 nm associated with NADH oxidation to NAD^+. Although this system was initially applied for kinetic characterization of the SAH hydrolase from *Bradyrhizobium elkanii*, the coupled reaction cascade is readily adaptable for studying MTs.

Other assays have been tailored for specific MT subfamilies, including halide MTs (HMTs; E.C. 2.1.1.165). HMTs catalyze the transfer of a methyl group from a methyl halide to SAH, leading to the production of SAM. Tang *et al.* developed a high-throughput and quantitative iodide-based assay applied in the directed evolution of an HMT from *Arabidopsis thaliana*.[36] A vanadium-dependent chloroperoxidase from *Curvularia inaequalis* is used here to oxidize iodide to hypoiodous acid (HOI), which in turn oxidizes the chromogen 3,3′,5,5′-tetramethylbenzidine (TMB, Fig. 2-IV) to form a diimine product in the final step. This assay enabled continuous monitoring by following the absorbance change at 570 nm, which was reported to be directly proportional to iodide in the range from 5 to 400 μM. Notably, this assay is compatible with crude lysate due to only minimal interference from chloride ions, even at concentrations as high as 1 M.

Kermani *et al.* and Wang *et al.* developed nanozyme-based assays for DNA methyltransferase activity.[51,52] Both exploit peroxidase-mimicking nanomaterials (DNA/Ag–Pt nanoclusters or PtNPs/AgNPs) that oxidize TMB at 652 nm, with the methylation disrupting catalytic activity—either directly or *via* DpnI-mediated cleavage of methylated DNA linkers on magnetic beads—achieving LODs of 0.05 U mL^{-1} (linear: 0.5–10 U mL^{-1}) and 0.4 U mL^{-1} (linear: 0.2–2 U mL^{-1}), respectively.

2.2. Fluorometric assays

Fluorescence is the emission of a photon when a molecule relaxes from an excited singlet state, produced from excitation

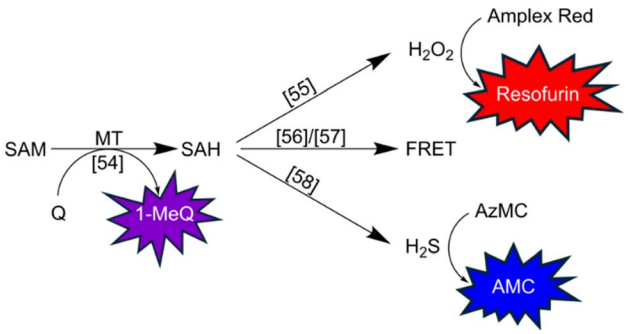

Fig. 3 Fluorometric assays for determining SAM-dependent methyltransferase activity. Example I: quinoline (Q) is converted to 1-methylquinoline (1-MeQ).[54] Example II: enzyme-coupled detection of SAH *via* peroxidase catalyzed oxidation leading to the formation of resofurin.[55] Example III/IV: Fluorescence resonance energy transfer (FRET)-based detection using riboswitch[56] and RNA aptamers,[57] respectively. Example IV: enzyme-coupled hydrogen sulfide formation with subsequent conversion of 7-azido-4-methylcoumarine (AzMC) to 7-amino-4-methylcoumarine (AMC).[58]

by photon absorption, back to the ground state. The emitted light is typically of lower energy than the absorbed light, due to non-radiative relaxation processes.[42,53] This principle has been used for the detection of MT reactions (Fig. 3).

Neelakantan *et al.* reported an *N*-MT specific assay that provides a direct und quantitative readout of *N*-MT activity using quinoline as the substrate.[54] Upon methylation, quinoline is converted to 1-methylquinoline (1-MeQ, Fig. 3-I), which exhibits intrinsic fluorescence. The product can be detected at 405 nm emission using an excitation wavelength of 330 nm. Unlike luminescence-based assays, this method does not require additional enzymatic cascades or needs to rely on the degradation of SAH. Consequently, the fluorescent signal correlates directly and quantitatively with the activity of the *N*-MT, offering a straightforward detection strategy, however the assay is limited to this specific substrate.

Akhtar *et al.* reported a substrate-independent fluorescence assay for MT activity.[55] In this system, SAH is hydrolyzed to adenine and L-homocysteine by a SAH nucleosidase. Adenine is then sequentially oxidized to 8-hydroxyadenine and 2,8-dihydroxyadenine, catalyzed by a xanthine oxidase. Both steps generate hydrogen peroxide (H_2O_2) as a by-product, which is utilized by a horseradish peroxidase (HRP) to oxidize the fluorescent probe Amplex Red into resorufin (excitation at 530 nm, emission at 590 nm, Fig. 3-II). This method provides a sensitive and quantitative readout for MT activity, as even low substrate turnover can be detected (0–20 μM).

Besides SAH degradation-based detection strategies, riboswitches can also be employed for MT assays. Pham *et al.*[56] developed a riboswitch-based SAH sensing assay, marketed as AptaFluor™, which utilizes a riboswitch from *Dechloromonas aromatica*. Upon binding SAH, the riboswitch undergoes a conformational change, which triggers fluorescence resonance energy transfer (FRET, Fig. 3-III). The authors reported that AptaFluor™ can detect SAH concentration as low as 10 nM and the assay is applicable to a wide range of MTs such as DNA-, RNA-, histone- and nucleosome-MTs. The assay is compatible with high-throughput screening, as it can be performed in a 384-well format with a total reaction volume of 10 μL. Importantly, the system is sensitive enough to detect MTs with SAM K_m value < 1 μM, indicating high affinity. Furthermore, the assays EC_{80} value (the optimal enzyme concentration, yielding robust signals under initial velocity conditions) is below 100 nM, making it suitable for the accurate determination of IC_{50} values of inhibitors. Building on the riboswitch-based assay, Nidoieva *et al.*[57] developed a SAH-sensing FRET RNA aptamer assay (Fig. 3-IV). Similar to the commercial AptaFluor™ system, their assay employes a 68-nucleotide RNA aptamer, which was identified upstream of the metH gene in *Dechloromonas aromatica*. Two aptamers, aptaSAH1 and aptaSAH2, were engineered and labeled with the FRET pair fluorescein (FAM) and tetramethylrhodamine (TAMRA). Their system exhibits high affinity for SAH even in the presence of SAM (K_D: 18 nM SAH and 5.3 μM SAM) making it suitable for detection of low SAH concentrations. In contrast to Pham *et al.*, Nidoieva *et al.* emphasized that their assay is approximately 100-fold cheaper per reaction ($0.05 to $5) than the assay of Pham *et al.* and provides full access to the aptamer sequence, enhancing transparency and reproducibility.

Recently, Menke *et al.* reported a fluorescence-dependent SAH detection assay applicable to crude lysates (Fig. 4). In this cascade, SAH is hydrolyzed by SAHH to yield L-homocysteine and adenosine. L-Homocysteine is further degraded to ammonia, α-ketobutyrate and hydrogen sulfide by a homocysteine-α-γ-lyase.[58] The hydrogen sulfide thus formed reduces 7-azido-4-methylcoumarine (AzMC) to 7-amino-4-methylcoumarine (AMC) which is fluorescent (excitation at 365 nm, emission at 450 nm). The authors reported that their assay reaches a maximum velocity at 500 μM SAH; therefore, if a MT produces SAH at higher rates, dilution steps are required to avoid saturation. A noted limitation is interference when analyzing *O*-MTs, as their products exhibit absorption maxima similar to the fluorescent AMC. The authors suggested that this issue can be mitigated by substituting AzMC with an alternative sulfide-sensitive probe. In early 2026, Chapple *et al.* presented the first continuous, uncoupled fluorescence-based assay for monitoring SAM-dependent MT activity, based on direct detection of proton release during methylation.[59] The method relies on a pH-shift principle, where proton generation during enzyme-catalyzed methyl transfer is detected using the pH-

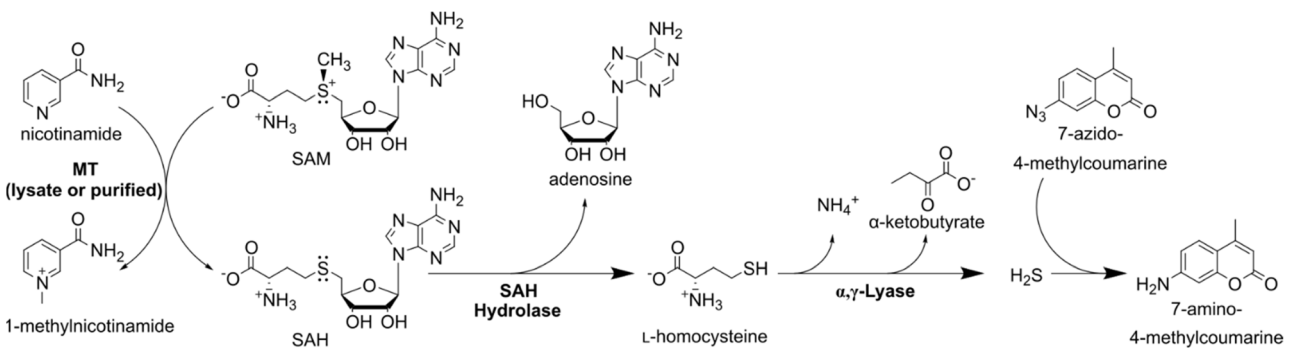

Fig. 4 Fluorometric assay for SAM-dependent methyltransferase activity, showing SAH formation from SAM *via* substrate methylation.[58] The SAH hydrolase cleaves SAH into L-homocysteine and adenosine. Further conversion by the homocysteine α,γ-lyase releases hydrogen sulfide (H_2S) enabling selective fluorescent detection through reduction of 7-azido-4-methylcoumarin (AzMC) to 7-amino-4-methylcoumarin (AMC). Formation of AMC can be quantified continuously by fluorescence measurements (λ_{exc}: 365 nm, λ_{em}: 450 nm) or by absorbance at 365 nm.

sensitive fluorescent probe pyranine (8-hydroxypyrene-1,3,6-trisulfonic acid). Changes in proton concentration shift pyranine's protonation equilibrium, resulting in a decrease in the fluorescence intensity ratio (F_{450}/F_{405}), which enables continuous monitoring of enzyme activity. The assay was validated on three representative MTs with different acceptor atoms—*N*-MT SgPsmC (*Streptomyces griseofuscus*), *O*-MT RnCOMT (*Rattus norvegicus*), and *C*-MT SrCouO (*Streptomyces rishiriensis*)—and showed sufficient correlation with HPLC-derived initial rates. Detection limits were in the low micromolar range (~4–12 μM LOD; ~11–36 μM LOQ). Despite advantages such as being enzyme-uncoupled, high-throughput compatible, and applicable to crude lysates or pre-treated whole cells, the method is constrained by its dependence on pH: sensitivity to buffering conditions and substrate pK_a necessitates careful calibration, accuracy for absolute quantification decreases over time due to system drift within a limited operational pH window (~6–8), and susceptibility to background proton fluctuations should be taken into account, especially with crude lysate of whole cell workflows.

2.3. Bioluminescence assays

Bioluminescence is a well-known phenomenon in which light is emitted by fireflies and other organisms. Depending on the organism, different mechanisms have been reported and the principle is widely exploited in biotechnology with the enzymatic turnover of D-luciferin by luciferase being most commonly used.[60] Through a distinct two-step mechanism catalyzed by the luciferase enzyme, D-luciferin is transformed into excited oxyluciferin under the consumption of ATP, which relaxes by releasing a photon (Fig. 5). This transformation requires (i) activation of the carboxylic group through adenylation to luciferyl-adenylate, and (ii) oxidation to the excited oxyluciferin.[60–62]

By utilizing this unique mechanism, very low levels of ATP (as low as 1.1×10^{-11} M) can be reliably detected in a linear manner.[60,63,64] In 2010, Ibáñez *et al.* reported a luciferin-ATP dependent assay, in which a degradation cascade was utilized to transform SAH into ATP, subsequently detected by the luciferase/D-luciferin system (Fig. 5-I).[65] SAH is first converted into adenine *via* 5′-methylthioadenosine/SAH nucleosidase (MTAN). Adenine is then transformed into adenosine monophosphate (AMP) through the action of an adenosine phosphoribosyl-transferase (APRT). Finally, AMP is phosphorylated to ATP through a pyruvate orthophosphate dikinase (PPDK) which serves as the cofactor for the luciferase/D-luciferin reaction. The authors aimed to develop a bioluminescence-based high-throughput assay to characterize the methylation of proteins through a protein methyltransferase (PMT). This assay is capable to detect SAH concentrations as low as 60 nM in a linear fashion in endpoint and continuous mode, and it is compatible with 96- and 384-well microplate formats.

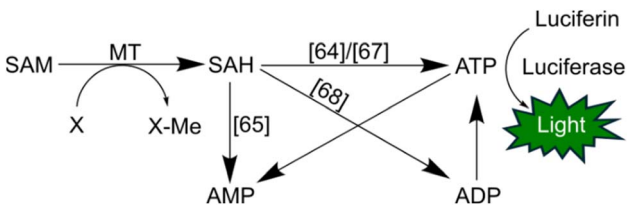

Fig. 5 Bioluminescence assays for determining SAM-dependent methyltransferase activity. Example I/III: SAH-to-ATP enzyme cascade for luminescent detection.[64,67] Example II: SAH degradation to AMP under ATP consumption.[65] Example IV: SAH-to-ATP formation *via* ADP.[68]

An alternative approach to detecting MT activity is based on measuring decreasing ATP levels by luminescence, which results in reduced signal intensity. Drake *et al.* developed an enzyme-coupled assay, in which SAH is degraded to AMP under ATP consumption (Fig. 5-II).[66] In this cascade, SAH is cleaved to adenosine by SAHH, differing from the pathway by Ibáñez *et al.* Adenosine is then converted to AMP by an adenosine kinase, consuming ATP in this process. The reduction in ATP concentration is quantified by the luciferase/D-luciferin reaction, where decreasing luminescence corresponds to higher MT activity. Drake *et al.* applied this assay to identify inhibitors of the histone NSD1 MT, which plays a significant role in leukemia.[66,67]

In 2016, Hsiao *et al.* published a bioluminescence-based assay for the detection of SAM-dependent MTs, which is commercially available as the MTase-GloTM.[68] Their assay operates through two distinct steps: in the first stage, the MT-Glo assay kit is used, in which SAHH hydrolyzes SAH to adenosine. An adenosine kinase (AdK) then phosphorylates adenosine to AMP. Using a polyphosphate AMP-phosphotransferase and guanosine triphosphate as a phosphate donor, AMP is converted to adenosine diphosphate (ADP). In the second stage (MTase-Glo detection solution), a pyruvate kinase converts ADP to ATP using phosphoenolpyruvate. The resulting ATP is quantified *via* the luciferase/D-luciferin reaction, producing a luminescent signal (Fig. 5-III). The authors reported that the assay can detect SAH concentrations as low as 20–30 nM. However, the system requires ultra-pure SAM to avoid false positive signals, since contaminating SAH can trigger background luminescence. The commercial provider claims that their SAM preparation generates 5–10-fold lower background compared to other commercial sources.

Dong *et al.* demonstrated that MT-catalyzed reactions can be detected either by fluorescence or luminescence, both relying on the by-product SAH.[69] In their approach, SAH can be processed through two alternative pathways: in the luminescent pathway, SAH is converted to ADP *via* the MTase-Glo cascade, ultimately leading to ATP formation and detection by the luciferase/D-luciferin system (Fig. 5-IV). In the fluorescence pathway, SAH is hydrolyzed to L-homocysteine, which subsequently reacts with a fluorescent probe to generate a measurable signal. Since SAHH is the key enzyme for this reaction, both detection strategies could, in principle, be performed in a single-pot approach. However, potential interference of the fluorescent and luminescent probe needs to be evaluated when this assay principle is applied.

2.4. Other assays

Beyond these widely employed spectrophotometric, fluorescence, and luminescence methods, several complementary assays have also been reported in literature. These include electrochemical methods, liquid chromatography coupled with mass spectrometry (LC-MS), and biosensor platforms. In the following section, we provide a brief overview of these assay formats.

As biosensors provide a rapid, sensitive and real-time detection, they are highly advantageous for the detection of enzymatic activity within living cells or extracts. They facilitate continuous and simultaneous screening of large enzyme variant libraries without the need for time-consuming sample preparation, enabling faster identification of optimal enzyme variants. For example, Zhen *et al.* engineered an L-homocysteine biosensor for *in vivo* use with *Arabidopsis thaliana* caffeic acid 3-*O*-MT, where UV-excitable GFPuv fluorescence correlated with L-homocysteine up to 0.1 mM. Alternatively, GFPuv can be substituted with LacZ for X-gal staining.[70]

LC-MS enables label-free detection by directly analysing the substrates and products of enzymatic reactions. This obviates the need for enzyme-coupling steps, allowing precise identification and quantification of chemical compounds based on their chromatographic retention times and molecular mass, thereby enabling to distinguish between mono and multiple methylated sites. Salyan *et al.* developed a LC-MS based assay to monitor the conversion of SAM to SAH, applying it to COMT with various known and potential substrates.[71] Notably, their assay is compatible with crude cell lysate, requiring no extraction steps and sample preparation involved only reaction quenching with formic acid, centrifugation to remove debris, and direct analysis of the resulting supernatant by LC-MS. Furthermore, the assay is applicable for kinetic measurements with its high sensitivity allowing for detection of SAH concentrations as low as 50 nM. For COMT, this high sensitivity enables activity screening before inhibitory SAH concentrations are reached. However, due to the time required for chromatographic separation and sample preparation, LC-MS is comparatively low in throughput (*e.g.* nine minutes per run in the assay mentioned before). The regioselectivity of methyltransferases can be directly assessed by LC-MS/MS through diagnostic fragmentation patterns—such as the position-specific $[M + H–CH_4]^+$ ion and retro-Diels-Alder fragments used to discriminate methylated flavonol regioisomers—though authentic reference standards are still required for unambiguous confirmation.[72] The use of deuterium-labeled *S*-adenosylmethionine as a methyl donor can further aid site assignment.[73] Where reference standards are unavailable and fragmentation patterns alone cannot unambiguously distinguish between possible regioisomers, NMR remains the gold standard for definitive regioselectivity assignment.[74] Emerging microfluidic technologies coupled with MS show promise for overcoming traditional LC-MS throughput limitations.[75] By enabling accelerated analysis in droplet or continuous-flow formats, these integrated systems can reduce reagent consumption while maintaining the advantages of label-free detection with MS.[76] Such approaches have demonstrated throughput increases by orders of magnitude, facilitating high-throughput screening applications.

3. Ongoing challenges and limitations

The vast selection of assays described in Section 2 indicates that no single assay can evaluate MT activity in a simple and accurate manner. Each assay has its advantages and limitations, which are the driving force for future developments in the field.

Photometric assays are simple to utilize and typically equipment is available in every laboratory. However, the absorbance detected should be in a spectral region where the background interference from the other molecules in the reaction mixture is minimal. A typical example is the use of Ellman's reagent which reacts with free thiols to provide a colourful product. As thiols are present in many proteins due to their cysteine residues, these side reactions can interfere with the activity measurements.[77] Substrate- or product-specific assays provide the advantage of well-defined absorbance spectra, but they are limited to specific reactions.

Fluorescence-based assays are versatile tools for the detection of MT activity, yet they exhibit certain limitations. Substrate-dependent assays (*e.g.* Neelakantan *et al.*[54]) may lead to false negatives, since not all MTs act on fluorogenic substrates, such as quinoline, potentially overlooking relevant enzymes. Hydrogen peroxide-dependent assays (*e.g.* Akhtar *et al.*[55]) require oxygen, thus they are unsuitable for oxygen-sensitive substrates. Moreover, the hydrogen peroxide produced might affect the enzyme. Cascade-based assays performed in crude lysate (*e.g.* Menke *et al.*[58]) circumvent the need for enzyme purification, but they face challenges such as saturation at high SAH concentrations (~500 μM) and potential spectral interference of fluorescent probes with the *O*-MTs products.

Bioluminescence-based assays for the detection of MTs offer high sensitivity, typically relying on ATP production to drive luciferase-catalyzed light emission. Nevertheless, as AMP, ADP and ATP are rather abundant in cellular environment, these assays are generally reliable only when applied with purified enzymes. Furthermore, ATP depletion assays, as the one presented by Drake *et al.*, is comparatively less reliable, since it remains unclear whether the observed decrease in ATP levels stems from AMP formation or from unrelated side reactions.[66]

In general, several of the assays discussed above rely on multi-enzymatic cascades. Such cascades should be designed to avoid long incubation times and to be applied in a continuous manner. Careful selection of the enzymes used in the cascade is required; for instance, enzymes with low K_m values to be able to detect low amounts of the intermediates, and enzymes that do not interfere with the intermediate products. Moreover, the enzyme ratio should be optimized, to ensure that the rate limiting step is the MT reaction.

A common limitation of all available high-throughput assays is their inability to determine regioselectivity (*i.e.*, when a substrate contains multiple hydroxyl groups, which could be methylated by an *O*-MT) or chemoselectivity (*i.e. N- vs. O-*

methylation). To get access to such information classical analytical techniques, such as LC-MS, are required; something that clearly reduces the throughput of the assay.

All previous remarks have to do with limitations of the assays. Nevertheless, we need to acknowledge another significant point on the usability of these assays. The assays monitor typically initial reaction rates of the MTs and enzymes are selected according to them; at this point enzymes perform their best. However, in a preparative reaction, enzyme stability and potential product inhibition are factors that could significantly affect the overall productivity. Utilization of downstream enzymes in the aforementioned assays to remove SAH (by degradation or SAM regeneration) works toward the alleviation of the potential inhibition of SAM-dependent MTs from the accumulation of SAH.[77,78] However, this strategy is usable only for the inhibition of the by-product of the reaction and does not help with the accumulation of the desired product, in case it also inhibits the MTs. Thus, the performance of the enzymes that are selected with high-throughput assays should be investigated under operational conditions, before selecting the most suitable biocatalyst for the process in design.

4. Future perspectives and promising technologies

In view of the above-discussed limitations, the development of next-generation screening strategies becomes essential. High-throughput compliant, automated (robotic) screening assays for MTs are a cornerstone for machine learning and artificial intelligence-based modelling.[79] The predictive power commonly increases with the size of properly generated data. For this purpose, MT assays should be conducted as comparable as possible. The collected data should contain evenly balanced property-enhancing and -reducing examples (to minimise bias); it should further be machine-actionable with rich metadata including the corresponding semantics. Recently, Weigmann *et al.* published a recommendation on best practices for automated high-throughput experiments.[80]

In particular, emerging technologies which enable more direct, sensitive, and potentially structure-informative readouts may help overcome current limitations. A promising road towards miniaturisation and parallelized automation of enzymatic assays is the utilisation of carbon materials, like graphene[81] and graphene oxide (GO),[82] as selective and highly sensitive electrode materials for direct measurement of enzymatic activities. In a similar manner, nano-technological applications, such as the nano-pore technology, offer miniaturised, highly sensitive, and parallelisable platforms for direct readouts.[83] Both technologies have the potential to address current gaps in enzymatic performance assessment.

Taken together, the integration of miniaturized and automated screening technologies, particularly the ones enabling more informative and direct readouts, is expected to significantly accelerate the development of robust and efficient MTs, while enabling the design and optimization of bioprocesses in industry-relevant settings.

5. Author contributions

The article was written jointly by all authors led by U. T. Bornscheuer and I. V. Pavlidis.

6. Conflicts of interest

There are no conflicts to declare.

7. Data availability

No primary research results, software or code have been included and no new data were generated or analysed as part of this review.

Supplementary information (SI) is available. See DOI: https://doi.org/10.1039/d6np00006a.

8. Acknowledgements

Florian Heinz acknowledges funding by a DBU PhD scholarship (AZ: 20024/038). Konstantin F. G. Weigmann and Mark Doerr gratefully acknowledge the financial support from the German Research Foundation, Germany (DFG) (grant number NFDI/2-1-2021) within the NFDI4Cat project to Uwe T. Bornscheuer. Renia Fotiadou and Ioannis V. Pavlidis acknowledge the European Union's HORIZON-WIDERA-2023-ACCESS-04 programme for the financial support under grant agreement 101159534 (WIDEnzymes). This manuscript reflects only the authors' views and opinions. Neither the European Union nor the granting authority can be considered responsible for them.

9. References

1 M. R. Bennett, S. A. Shepherd, V. A. Cronin and J. Micklefield, *Curr. Opin. Chem. Biol.*, 2017, **37**, 97–106.
2 J. Li, C. Sun, W. Cai, J. Li, B. P. Rosen and J. Chen, *Mutat. Res., Rev. Mutat. Res.*, 2021, **788**, 108396.
3 H. Luo, A. S. L. Hansen, L. Yang, K. Schneider, M. Kristensen, U. Christensen, H. B. Christensen, B. Du, E. Özdemir, A. M. Feist, J. D. Keasling, M. K. Jensen, M. J. Hårrgard and B. O. Palsson, *PLoS Biol.*, 2019, **17**, e2007050.
4 E. J. Barreiro, A. E. Kümmerle and C. A. Fraga, *Chem. Rev.*, 2011, **111**, 5215–5246.
5 Q. Tang, I. V. Pavlidis, C. P. S. Badenhorst and U. T. Bornscheuer, *ChemBioChem*, 2021, **22**, 2584–2590.
6 Y. Hao, Z. Wei, Z. Wang, G. Li, Y. Yao and B. Dun, *Foods*, 2021, **10**, 2367.
7 B. Ang, T. Yang, H. Jiang, Y. Cheng, Y. Chen, X. Qie, L. Yin, T. Wang, Q. Chen, Z. Wang, M. Zeng, B. Adhikari, Z. He and J. Chen, *J. Agric. Food Chem.*, 2025, **73**, 13973–13984.
8 L. Wen, Y. Jiang, J. Yang, Y. Zhao, M. Tian and B. Yang, *Ann. N. Y. Acad. Sci.*, 2017, **1398**, 120–129.
9 S. K. Shrestha, N. Ghimire, W. H. Lee, H. J. Kim and T. J. Oh, *Int. J. Biol. Macromol.*, 2025, **319**, 145520.
10 N. Koirala, N. H. Thuan, G. P. Ghimire, D. V. Thang and J. K. Sohng, *Enzyme Microb. Technol.*, 2016, **86**, 103–116.

11 S. Letchuman, H. D. T. Madhuranga, B. L. N. K. Madhurangi, A. D. Premarathna and M. Saravanan, *Intell. Pharm.*, 2025, **3**, 268–276.
12 R. Chen, M. Wang, J. D. Keasling, T. Hu and X. Yin, *Trends Biotechnol.*, 2024, **42**, 699–713.
13 J. P. Kanter, M. Ahlhorn, H. Zorn, B. Li and M. Gand, *J. Agric. Food Chem.*, 2025, **73**, 13594–13604.
14 A. Kunzendorf, B. Zirpel, L. Milke, J. P. Ley and U. T. Bornscheuer, *ChemCatChem*, 2023, **15**, e202300951.
15 E. H. Hansen, B. L. Møller, G. R. Kock, C. M. Bünner, C. Kristensen, O. R. Jensen, F. T. Okkels, C. E. Olsen, M. S. Motawia and J. Hansen, *Appl. Environ. Microbiol.*, 2009, **75**, 2765–2774.
16 K. Li and J. W. Frost, *J. Am. Chem. Soc.*, 1998, **120**, 10545–10546.
17 B. P. Chapple, L. Nitz, P. Schneider, B. Henssen, S. Myllek, M. Haase, T. Classen and J. Pietruszka, *Angew. Chem., Int. Ed.*, 2025, **65**, e15459.
18 A. W. Struck, M. L. Thompson, L. S. Wong and J. Micklefield, *ChemBioChem*, 2012, **13**, 2642–2655.
19 E. Abdelraheem, B. Thair, R. F. Varela, E. Jockmann, D. Popadić, H. C. Hailes, J. M. Ward, A. M. Iribarren, E. S. Lewkowicz, J. N. Andexer, P. L. Hagedoorn and U. Hanefeld, *ChemBioChem*, 2022, **23**, e202200212.
20 D. K. Liscombe, G. V. Louie and J. P. Noel, *Nat. Prod. Rep.*, 2012, **29**, 1238–1250.
21 Y. Fukumoto, R. Kyono, Y. Shibukawa, Y. K. Tanaka, N. Suzuki and Y. Ogra, *J. Biol. Chem.*, 2024, **300**, 105599.
22 J. W. Schmidberger, A. B. James, R. Edwards, J. H. Naismith and D. O'Hagan, *Angew. Chem., Int. Ed.*, 2010, **49**, 3646–3648.
23 X. Cheng, S. Kumar, J. Posfai, J. W. Pflugrath and R. J. Roberts, *Cell Press*, 1993, **74**, 299–307.
24 S. Duchin, Z. Vershinin, D. Levy and A. Aharoni, *Epigenet. Chromatin*, 2015, **8**, 56.
25 C. Ye, B. M. Sutter, Y. Wang, Z. Kuang and B. P. Tu, *Mol. Cell*, 2017, **66**, 180–193.
26 Q. Tang, Y. M. Vianney, K. Weisz, C. W. Grathwol, A. Link, U. T. Bornscheuer and I. V. Pavlidis, *ChemCatChem*, 2020, **12**, 3721–3727.
27 H. L. Schubert, R. M. Blumenthal and X. Cheng, *Trends Biochem. Sci.*, 2003, **28**, 329–335.
28 G. L. Cantoni, *Annu. Rev. Biochem.*, 1975, **44**, 435–451.
29 S. C. Lu, *Int. J. Biochem. Cell Biol.*, 2000, **32**, 391–395.
30 C. Zubieta, J. R. Ross, P. Koscheski, Y. Yang, E. Pichersky and J. P. Noel, *Plant Cell*, 2003, **15**, 1704–1716.
31 C. Zubieta, X. Z. He, R. A. Dixon and J. P. Noel, *Nat. Struct. Mol. Biol.*, 2001, **8**, 271–279.
32 I. Gómez García, C. E. Stevenson, I. Usón, C. L. Freel Meyers, C. T. Walsh and D. M. Lawson, *J. Mol. Biol.*, 2010, **395**, 390–407.
33 J. G. Kopycki, D. Rauh, A. A. Chumanevich, P. Neumann, T. Vogt and M. T. Stubbs, *J. Mol. Biol.*, 2008, **378**, 154–164.
34 P. Z. Kozbial and A. R. Mushegian, *BMC Struct. Biol.*, 2005, **5**, 19.
35 S. J. Booker and C. T. Lloyd, *ACS Bio Med Chem Au*, 2022, **2**, 538–547.
36 Q. Tang, C. W. Grathwol, A. S. Aslan-Üzel, S. Wu, A. Link, I. V. Pavlidis, C. P. S. Badenhorst and U. T. Bornscheuer, *Angew. Chem., Int. Ed.*, 2021, **60**, 1524–1527.
37 T. D. Huber, B. R. Johnson, J. Zhang and J. S. Thorson, *Curr. Opin. Biotechnol.*, 2016, **42**, 189–197.
38 L. Gericke, D. Mhaindarkar, L. C. Karst, S. Jahn, M. Kuge, M. K. F. Mohr, J. Gagsteiger, N. V. Cornelissen, X. Wen, S. Mordhorst, H. J. Jessen, A. Rentmeister, F. P. Seebeck, G. Layer, C. Loenarz and J. N. Andexer, *ChemBioChem*, 2023, **24**, e202300133.
39 A. Y. Rudenko, S. S. Mariasina, R. M. Ozhiganov, P. V. Sergiev and V. I. Polshakov, *Biochemistry*, 2025, **90**, S105–S134.
40 T. D. Huber, F. Wang, S. Singh, B. R. Johnson, J. Zhang, M. Sunkara, S. G. Van Lanen, A. J. Morris, G. N. Phillips Jr and J. S. Thorson, *ACS Chem. Biol.*, 2016, **11**, 2484–2491.
41 J. Axelrod and H. Weissbach, *J. Biol. Chem.*, 1961, **236**, 211–213.
42 F. Hinderer, *Uv/vis-Absorptions- Und Fluoreszenz-Spektroskopie*, Springer Fachmedien Wiesbaden GmbH, Wiesbaden, Germany, 1 edn, 2020.
43 R. T. Borchardt, *Anal. Biochem.*, 1974, **58**, 382–389.
44 C. L. Hendricks, J. R. Ross, E. Pichersky, J. P. Noel and Z. S. Zhou, *Anal. Biochem.*, 2004, **326**, 100–105.
45 T. F. Schäberle, C. Siba, T. Höver and G. M. König, *Anal. Biochem.*, 2013, **432**, 38–40.
46 K. M. Dorgan, W. L. Wooderchak, D. P. Wynn, E. Karschner, J. F. Alfaro, Y. Cui, Z. S. Zhou and J. M. Hevel, *Anal. Biochem.*, 2006, **350**, 249–255.
47 H. Simon-Baram, S. Roth, C. Niedermayer, P. Huber, M. Speck, J. Diener, M. Richter and S. Bershtein, *ChemBioChem*, 2022, **23**, e202200162.
48 J. T. Nelson, J. Lee, J. W. Sims and E. W. Schmidt, *Appl. Environ. Microbiol.*, 2007, **73**, 3575–3580.
49 B. Rohde, J. Hans, S. Martens, A. Baumert, P. Hunziker and U. Matern, *Plant J.*, 2008, **53**, 541–553.
50 L. L. Kailing, D. Bertinetti, F. W. Herberg and I. V. Pavlidis, *New Biotechnol.*, 2017, **39**, 11–17.
51 H. A. Kermani, M. Hosseini, A. Miti, M. Dadmehr, G. Zuccheri, S. Hosseinkhani and M. R. Ganjali, *Anal. Bioanal. Chem.*, 2018, **410**, 4943–4952.
52 C. Wang, L. Jiang, Y. Zaho, L. Cheng, L. Zhou, A. Liu and L. Xu, *Sens. Actuators, B Chem.*, 2025, **429**, 137298.
53 M. L. Martínez, P. Marín-Rosas, V. B. López-Cervantes, A. Guzmán-Vargas, R. A. Peralta, D. Solis-Ibarra and I. A. Ibarra, *Dalton Trans.*, 2025, **54**, 13806–13819.
54 H. Neelakantan, V. Vance, H. L. Wang, S. F. McHardy and S. J. Watowich, *Biochemistry*, 2017, **56**, 824–832.
55 M. K. Akhtar, D. Vijay, S. Umbreen, C. J. McLean, Y. Cai, D. J. Campopiano and G. J. Loake, *Front. Bioeng. Biotechnol.*, 2018, **6**, 146.
56 H. Pham, M. Kumar, A. R. Martinez, M. Ali and R. G. Lowery, *SLAS Discovery*, 2024, **29**, 100161.
57 Z. Nidoieva, M. O. Sabin, T. Dewald, A. C. Weldert, S. N. Hoba, M. Helm and F. Barthels, *Commun. Chem.*, 2025, **8**, 32.
58 M. J. Menke, P. Schneider, C. P. S. Badenhorst, A. Kunzendorf, F. Heinz, M. Dörr, M. A. Hayes and

U. T. Bornscheuer, *Angew. Chem., Int. Ed.*, 2023, **62**, e202313912.
59 B. P. Chapple, L. M. Böhmer and J. Pietruszka, *ChemCatChem*, 2026, **18**, e01714.
60 A. J. Syed and J. C. Anderson, *Chem. Soc. Rev.*, 2021, **50**, 5668–5705.
61 J. A. Koo, S. P. Schmidt and G. B. Schuster, *Proc. Natl. Acad. Sci. U. S. A.*, 1978, **75**, 30–33.
62 B. R. Branchini, C. E. Behney, T. L. Southworth, D. M. Fontaine, A. M. Gulick, D. J. Vinyard and G. W. Brudvig, *J. Am. Chem. Soc.*, 2015, **137**, 7592–7595.
63 T. Fukuba, Y. Aoki, N. Fukuzawa, T. Yamamoto, M. Kyo and T. Fujii, *Lab Chip*, 2011, **11**, 3508–3515.
64 C. B. Hansen, A. Kerrouche, K. Tatari, A. Rasmussen, T. Ryan, P. Summersgill, M. P. Y. Desmulliez, H. Bridle and H. J. Albrechtsen, *J. Microbiol. Methods*, 2019, **165**, 105713.
65 G. Ibáñez, J. L. McBean, Y. M. Astudillo and M. Luo, *Anal. Biochem.*, 2010, **401**, 203–210.
66 K. M. Drake, V. G. Watson, A. Kisielewski, R. Glynn and A. D. Napper, *Assay Drug Dev. Technol.*, 2014, **12**, 258–271.
67 J. Wang, N. Liao, G. Liu, Y. Li, F. Xu and J. Shi, *Crit. Rev. Biotechnol.*, 2024, **44**, 1203–1225.
68 K. Hsiao, H. Zegzouti and S. A. Goueli, *Epigenomics*, 2016, **8**, 321–339.
69 G. Dong, A. Yasgar, D. L. Peterson, A. Zakharov, D. Talley, K. C. Cheng, A. Jadhav, A. Simeonov and R. Huang, *ACS Comb. Sci.*, 2020, **22**, 422–432.
70 Z. Zhen, L. Xiang, S. Li, H. Li, Y. Lei, W. Chen, J. M. Jin, C. Liang and S. Y. Tang, *Biosens. Bioelectron.*, 2025, **268**, 116904.
71 M. E. Salyan, D. L. Pedicord, L. Bergeron, G. A. Mintier, L. Hunihan, K. Kuit, L. A. Balanda, B. J. Robertson, J. N. Feder, R. Westphal, P. A. Shipkova and Y. Blat, *Anal. Biochem.*, 2006, **349**, 112–117.
72 C. Ma, H. Lv, X. Zhang, Z. Chen, J. Shi, M. Lu and Z. Lin, *Anal. Chim. Acta*, 2013, **795**, 15–24.
73 C. Li, A. Schmidt, E. Pichersky, F. Shi and A. D. Jones, *Metabolomics*, 2012, **9**, 92–101.
74 S. Darsandhari, D. Dhakal, B. Shrestha, P. Parajuli, J. H. Seo, T. S. Kim and J. K. Sohng, *Enzyme Microb. Technol.*, 2018, **113**, 29–36.
75 X. W. Diefenbach, I. Farasat, E. D. Guetschow, C. J. Welch, R. T. Kennedy, S. Sun and J. C. Moore, *ACS Omega*, 2018, **3**, 1498–1508.
76 R. Kurita and O. Niwa, *Lab Chip*, 2016, **16**, 3631–3644.
77 J. H. Lin, C. W. Chang, Z. H. Wu and W. L. Tseng, *Anal. Chem.*, 2010, **82**, 8775–8779.
78 C. Liao and F. P. Seebeck, *Nat. Catal.*, 2019, **2**, 696–701.
79 N. Singh, S. Lane, T. Yu, J. Lu, A. Ramos, H. Cui and H. Zhao, *Nat. Commun.*, 2025, **16**, 5648.
80 K. F. Weigmann, U. T. Bornscheuer and M. Doerr, *Curr. Opin. Biotechnol.*, 2025, **97**, 103395.
81 I. V. Pavlidis, M. Patila, U. T. Bornscheuer, D. Gournis and H. Stamatis, *Trends Biotechnol.*, 2014, **32**, 312–320.
82 H. Jang, J. Lee and D. H. Min, *J. Mater. Chem. B*, 2014, **2**, 2452–2460.
83 S. Zhang, W. Shi, K. B. Li, D. M. Han and J. J. Xu, *Anal. Chem.*, 2022, **94**, 4407–4416.

